Theor. Appl. Climatol. 79, 31–43 (2004)
DOI 10.1007/s00704-004-0071-6

Theoretical and Applied Climatology
Printed in Austria

[1] Department of Atmospheric Sciences, Lanzhou University, Lanzhou, China
[2] Geophysical Institute, University of Alaska Fairbanks, Fairbanks, AK, USA
[3] Department of Mathematics, Wuhan University, Wuhan, China
[4] Chinese Academy of Meteorological Sciences, Beijing, China

A coupled simple climate model and its global analysis

X. Fan[1,2,4], **J.-F. Chou**[1], **B.-R. Guo**[3], and **M. D. Shulski**[2]

With 3 Figures

Received February 6, 2003; revised February 13, 2004; accepted May 7, 2004
Published online July 29, 2004 © Springer-Verlag 2004

Summary

An atmosphere-land coupled simple climate model is constructed and its climatic properties are analyzed by introducing a global analysis method, cell mapping. The simple model is a nonlinear six order simplified climate model featured with chaotic dynamics, dissipation, and forcing source, which are the main features of the real climate system. The cell mapping method is applied with this coupled system. Numerical experiments are carried out for investigating the interactions between the fast-changing atmospheric variables and slow-changing underlying surface variables. The predictability of the system is also investigated via the global analysis, with which the evolution of the system is translated to the evolution of probability transition on a Markov Chain. An effective scheme is proposed for computing the probability transition matrix for the coupled system. Predictions can be made based on the combination of dynamics and statistics. The importance of constructing the coupled model is shown by globally analyzing the predictability of the coupled system. The coupling mechanism prolongs the memorization of initial information, and then the predictability as well.

1. Introduction

Lorenz revealed first in 1963 (Lorenz, 1963) that there may exist an indeterminate state in a perfectly deterministic nonlinear system because of initial error. Lorenz also found chaotic solution in his Hadley circulation system model and pointed out that the long-term behavior of the system was of indeterminacy (Lorenz, 1984). In terms of long-term behavior of chaotic systems, Chou (1983, 1986, 1987, and 1989) has explored atmospheric system models from the view point of geometrical visualization and pointed out that there exists an asymptotic state for the atmospheric system, which is regarded as the strange attractor.

With the help of geometrical visualization, Chou (1995) discovered the fact that the dynamic atmospheric equation set is actually a very special operator equation in the Hilbert space. A nonlinear system with forcing and dissipation has been revealed to have several attractors in the state space. The attractors are distributed in a finite area and each is a set of points of zero volume within an attracting region of non-zero volume. Any system state must be within the attracting region of a certain attractor and tends to the attractor with time. Chou (1995) has also reviewed the work in the area of nonlinear climate dynamics and concluded that chaotic systems need global analysis of long term asymptotic state, which is also considered a new important feature of the climate system.

For global analysis, Nicolis (1990) put forward the "coarse graining" or "lumping" method to display the global evolution of a chaotic system and to carry out statistical prediction. However, it is difficult to obtain a priori knowledge of invariant probability for atmospheric dynamic systems, which is needed to determine the transition probability matrix of a Markov Chain. Hsu (1980, 1981, and 1982) raised another global analysis method, cell-to-cell mapping, for use in various dynamic systems. Guo et al. (1996) and Zhang et al. (1998, hereafter Zhang98) have successfully applied this method to their simplified climate system.

By applying the cell-to-cell mapping method to a simplified climate model, Zhang98 has demonstrated the benefits and advantages of utilizing simplified models and of introducing new mathematical methods in climate study. However, the simplified model in Zhang98 is of an atmospheric model and contains only fast-changing atmospheric variables. As illustrated by Zhang98, the behavior of this system varies with external parameters, especially the surface temperatures $(T_1)_4$, $(T_2)_4$ and $(T_3)_4$ (see also Section 2), which are slow-changing variables.

In fact, the climate system contains movements of different kinds of mediums dependent upon their heat capacity. Particularly, the air mass has small heat capacity and it is a fast changing component, while the underlying surface (either land or ocean) has larger heat capacity and it is a relatively slow-changing component in the climate system. There are interactions between the components, which may be influenced or controlled by external parameters.

The objective of this paper is to construct a coupled system in which different kinds of components, at least two, are contained, so that more properties of the climate system could be revealed, especially the long-term behavior of both fast- and slow-changing variables, their interactions, and external force dependence. Specifically, a coupled system based on the Zhang98 simplified climate model will be constructed, in which the surface temperatures $(T_1)_4$, $(T_2)_4$ and $(T_3)_4$ are no longer external parameters, but state variables. The solar radiation term will be the external parameter which determines the ultimate chaotic state of the system.

In earlier classical studies of deterministic predictability, the deterministic prediction of subsequent evolution of atmospheric states is limited to a few days due to the presence of dynamical instabilities and nonlinear interactions (Lorenz, 1965, 1969, 1982; Charney et al., 1966; Smagorinsky, 1969), and the theoretical upper limit in general circulation models is determined by the growth rate and the magnitude of error between the two model evolutions for which the initial conditions differed by only a small random perturbation. Shukla (1981) studied the dynamical predictability of space and time averages based on the question raised by Charney and Shukla (1980). It was indicated that there is a physical basis to make dynamical prediction of monthly means at least up to one month, and that there still is the possibility, at least in principle, to extend the predictability limit even beyond one month by improving the model, the initial conditions, and the parameterizations of physical processes.

The cell mapping method will be used here to globally analyze the coupled climate system. An improved method for computing transition probability matrix for the coupled model has been put forward and been utilized to investigate the predictability of the system. Zhang98 has also shown the hope of extending the climate predictability if the effects of the land and ocean are coupled with the atmospheric model. This is another motivation of establishing a coupled model.

2. Simplified climate model

The simplified climate model in Zhang98 is a set of third order autonomous ordinary differential equations. Its vector form is:

$$\frac{d}{dt}\begin{bmatrix} X_1 \\ X_2 \\ X_3 \end{bmatrix} = \begin{bmatrix} 0 & a_{12}-\sigma_1 X_2 & a_{13}-\sigma_1 X_3 \\ \sigma_1 X_2 - a_{12} & 0 & a_{23}-\sigma_2 X_1 \\ \sigma_1 X_3 - a_{13} & \sigma_2 X_1 - a_{23} & 0 \end{bmatrix} \begin{bmatrix} X_1 \\ X_2 \\ X_3 \end{bmatrix} + \begin{bmatrix} a_{11} & 0 & 0 \\ 0 & a_{22} & 0 \\ 0 & 0 & a_{33} \end{bmatrix} \begin{bmatrix} X_1 \\ X_2 \\ X_3 \end{bmatrix} + \begin{bmatrix} b_1 \\ b_2 \\ b_3 \end{bmatrix} \tag{1}$$

where $\mathbf{X} = [X_1, X_2, X_3]^{\mathrm{T}}$ are dimensionless atmospheric variables that represents three spherical harmonic components of 500 hPa temperature,

a_{ij} ($i \neq j$) and b_i ($i,j = 1,2,3$) are functions of dimensionless underlying surface temperature $(\mathbf{T})_4 = [(T_1)_4, (T_2)_4, (T_3)_4]^T$ (also three spherical harmonic components), and a_{ii} ($i = 1,2,3$), σ_1 and σ_2 are constants. All of the coefficients and constants in the model (1) can be found in Zhang98. Given a set of $(\mathbf{T})_4$, [0.414336, −0.01243, −0.4870765], and an appropriate initial $\mathbf{X}$ (within the range shown in (2)–(4) below), this model can be steadily integrated to get the evolution of $\mathbf{X}$ (Zhang98), which falls on a chaotic attractor that lies in the domain of:

$$X_1 \in [-3.1188, -0.9422],\ X_2 \in [-2.0747, 0.4987],\ X_3 \in [-1.2103, 1.9749] \quad (2)$$

The state variables in Eq. (1) are the dimensionless atmospheric variables, so Eq. (1) is considered a nonlinear dynamic system in a general sense. Its asymptotic state is a chaotic attractor in the phase space as shown in Fig. 1a–c.

3. A coupled simple climate model

3.1 Model

The external forcing terms of the simplified climate model (1), b_1, b_2, and b_3 depends on $(T_1)_4$, $(T_2)_4$, and $(T_3)_4$, which are underlying surface temperatures as defined at the level 1000 hPa in the model (1). To better simulate the real climate

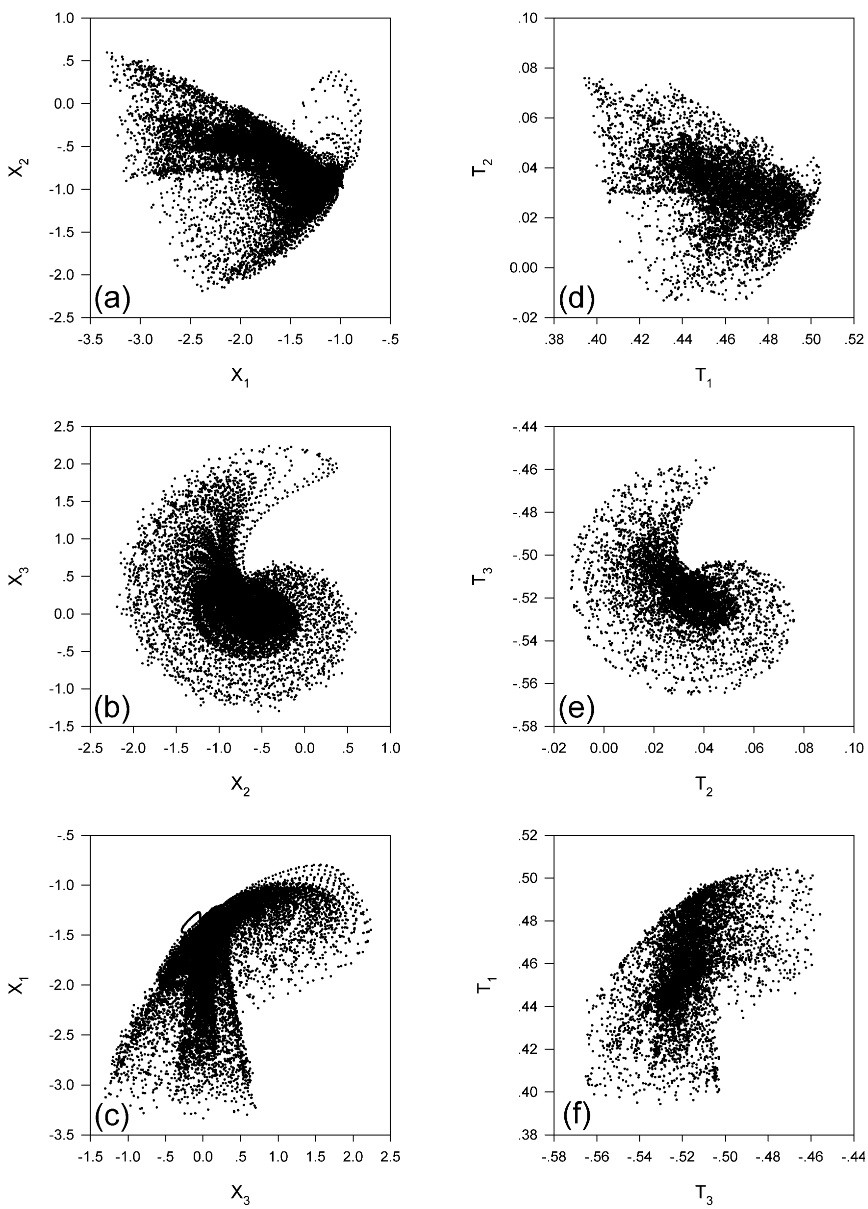

Fig. 1. Projections of the coupled model evolutions on planes X_1–X_2, X_2–X_3, X_3–X_1, T_1–T_2, T_2–T_3, and T_3–T_1 in phase space of the portion of the points between the years 101–120

with a simplified model, these underlying surface temperatures are also going to be considered as state variables. Therefore, a coupled simple climate model is constructed herein.

The underlying surface model is considered as a third boundary value problem of the linear thermal conductive equation. Guo et al. (1996) derived an analytical solution of the thermal conductive equation as (see Appendix):

$$T_S(0,t) = \sum_{i=1}^{n} F_1(0,t,\tau_i) f(\lambda,\theta,\tau_i) + \sum_{i=1}^{m} F_2(0,t,\zeta_i) T_S(\zeta_i,0) \quad (3)$$

where $T_S(0,t)$ represents surface temperatures $(T_1)_4$, $(T_2)_4$, and $(T_3)_4$; $f(\lambda,\theta,\tau_i)$ is the boundary condition term which stands for the influences from the atmosphere; $T_S(\zeta_i,0)$ is initial soil temperature; and F_1 and F_2 are integral coefficients (Guo et al., 1996).

The models (1) and (3) compose a coupled nonlinear system. The coupling mechanism (see Appendix) is the energy balance at the interface between atmosphere and underlying surface (land or ocean). Now, in this coupled system, the unique external forcing is from solar radiation R_s. When the solar radiation is determined, the model evolves toward its attractor from a given initial point in phase space **X**–**T** ($\mathbf{T} = [T_1, T_2, T_3]^{\mathrm{T}}$, $(\ )_4$ is omitted hereafter).

3.2 Model performance

Based on the coupling mechanism of the coupled model and corresponding parameters and constants (see Appendix; Zhang98; Guo et al., 1996), the model is integrated from the initial point $(X_1, X_2, X_3, T_1, T_2, T_3) = (-1.68078, -0.80321, 0.23754, 0.48165, 0.03022, -0.51504)$. The integral time step is 0.25 h. Due to the slow-changing characteristics of the variable **T**, model (3) is coupled once a day (96 time steps) with model (1). By taking 360 days as the period of solar radiation, which is also the model year (the first day starts from the winter solstice), the coupled model has been integrated for one thousand years. Figure 1 shows the projections on X_1–X_2, X_2–X_3, X_3–X_1, T_1–T_2, T_2–T_3 and T_3–T_1 planes in the phase space of the portion of the points corresponding to the days between the year 101 to 120. The results show clearly a chaotic attractor in the **X**–**T** space, lying in the **X** domain of (2) and **T** domain of:

$$T_1 \in [0.38567, 0.51203], T_2 \in [-0.01997, 0.08647], T_3 \in [-0.57118, -0.44552]. \quad (4)$$

The domains (2) and (4) determine the attractor area in the 6-dimensional phase space.

Here presents further discussions about other features of the model and reflections of the real climate system within this simple system.

i) The coupled model is computationally effective such that a large amount of numerical experiments could be performed. As shown by Zhang98 and the experiments in section 5, the generalized cell mapping can be used with this model. To introduce new mathematical theories and methods for studying climate is one of our original purposes of building this model.
ii) From the standpoint of physics, the coupled system retains basic features of the real climate system, while the complex physical processes and their mathematical equations are simplified. These features include a chaotic attractor as shown in Fig. 1, nonlinear interactions between fast- and slow changing components, dissipative effects, and external forcing. Figure 2 shows the time series of each variable, from which the fast-changing **X** variables and slow-changing **T** variables are illustrated.
iii) Figures 1 and 2 shows qualitatively the chaotic character of the model evolution. Generally, there are several statistic values that have been used to quantitatively depict a chaotic system, such as fractal dimension, Lyapnov index, graduation index, and power spectrum index (Thompson and Stewart, 1986). Among them, the fractal dimension indicates the complexity (or nonperiodicity) of a system. According to Guo et al.'s (1996) calculation, the simple atmospheric model's fractal dimension varies from 1.04 to 2.33 for different underlying surface temperatures. These results reveal that the chaotic character of the atmosphere is affected significantly by land surface, which acts as the external forcing for the atmosphere. The results also imply that the interaction of the atmosphere

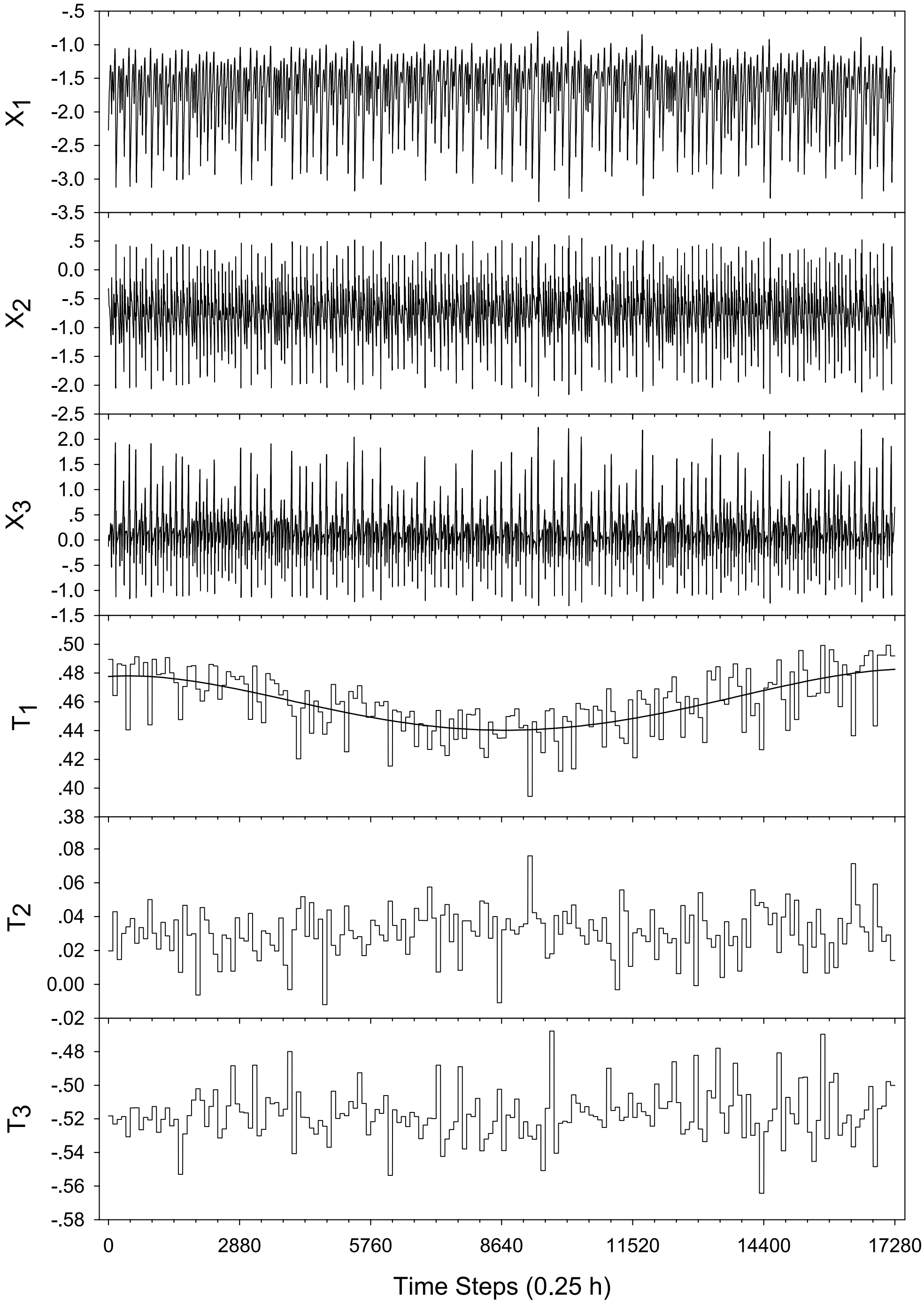

Fig. 2. Time series of variables X_1, X_2, X_3, T_1, T_2, and T_3 during the first half of the year 101

and the land surface in the coupled simple system is complex, which is helpful in our study of complex climate states. The results of Lyapnov index and power spectrum index of Guo et al. (1996) provide proofs that the simple coupled system is sensitive to initial conditions and has a strange chaotic attractor. Long-term evolution of the model tends to the chaotic attractor. The chaotic attractor, i.e. chaotic states, is the destination of all states started from all initial points after a long-term evolution. In other words, the chaotic states are final states of the system when all initial information has been completely lost, which is the climate states. Therefore, studying long-term behavior and the chaotic states is a way to study the climate. This leads to a new definition of climate based on chaotic dynamics: climate is a probability distribution of state variables on chaotic attractor determined by certain external forcing (or control variables).

iv) The simple coupled model has been built intentionally to have chaotic solution. Since it is mostly simplified, some of the constants and parameters are allowed to be out of their physical value ranges (Guo et al., 1996). For example, as shown in Zhang98, the model requires the variable **T** to be in the domain of (4). In addition, due to the assumption of symmetry of the northern and southern hemispheres (Zhang98), the model has a half year period of change instead of one year in regard to the solar radiation (see Fig. 2). Nevertheless, the periodic component is illustrated in variable T_1, besides the chaotic evolution in all the six variables.

v) The results from Figs. 1 and 2 also imply that there exists three kinds of time scales in this coupled system: 1) long periodic changes of external forcing of solar radiation; 2) slow changes of underlying land surface temperature controlled by solar radiation; and 3) fast adjustment processes of atmospheric variables to the chaotic attractor determined by land surface temperatures. This is another major feature of the real climate system that is reflected from this simplified nonlinear coupled model.

From the above discussion, the simplified climate model possesses the basic features of the real climate system and can be use to perform adequate numerical experiments to study basic problems of climate.

4. Global analysis method: cell mapping

Cell mapping method is put forward to globally analyze nonlinear systems (Hsu, 1987). As can be seen, discretization transforms have been carried out during all the previous simplifying processes from continuous partial differential equations to ordinary differential equations, and then to difference equations. They are all discretizations with respect to the independent spatial and temporal variables. The dependence of dependent variables on the independent variables has never been changed. It is still continuous in terms of mapping; however, all the dependent variables are actually discretized in a computer due to the limited word-length of a computer.

4.1 Simple cell mapping: a global analysis to round-off error

According to Hsu (1987), the phase space of a model running on a computer is divided into small cells with side-length equals to the computer word-length (i.e. round-off error) and turns into a cell space. Any model state in a computer goes from one cell to another in one time step. Obviously, the dynamical system in the cell space is still a deterministic system provided the modeling never overflows. Each cell has only one image cell of mapping. This is called simple cell mapping (Hsu, 1987).

In terms of simple cell mapping, the long-term global property of a dynamic system is featured by its periodic solution in the cell space. For a given system running on a computer, the total number of cells is finite, say N. There are two kinds of cells in the cell space, periodic and transient cells. A periodic cell returns to itself after a finite number of mapping steps and a transient cell never returns to itself, but indeed, goes to periodic cells after finite mapping steps. Obviously, there are at least one and at most N periodic solutions in a cell space. Therefore, the chaotic attractor is also a periodic solution despite its period being very long.

Under the concept of simple cell mapping, the impact of round-off error of computation has been eliminated. With the aid of simple cell mapping, the long-term asymptotic behavior, i.e. the climate is determined by the probability distribution on all periodic cells. The uncertainty of individual points turns into certainty in a simple cell, and the system evolution is deterministic.

4.2 Generalized cell mapping: a global analysis to observational error

Generalized cell mapping has been used diversely in nonlinear system analysis since Hsu (1980) first put forward the method (Hsu, 1981, 1982, 1987; Hsu et al., 1980, 1982; Zhang98; Guo et al., 1996). It has been applied by Zhang98 to the simplified atmospheric model and its advantages in global analysis and predictability study have been shown.

For any numerical model, the initial state of state variables is obtained from observation, of which the observational error is unavoidable and generally far greater than the round-off error. Subsequently, the simple cell space is divided into larger cells with side-length equal to the observational error and turns into the so-called generalized cell space. Each generalized cell has many simple cells and can have more than one image cell. Obviously, uncertainty of model evolution is unavoidable because it is impossible to know which simple cell is the true initial even if the generalized cell is given by the observation.

Assume there are a total of M generalized cells and the system state is in the generalized cell Q_j when $t = t_n$, the state at $t = t_{n+1}$ could fall in cell Q_1 with probability $p_{1,j}$, in cell Q_2 with probability $p_{2,j}, \ldots$, and in cell Q_i with probability $p_{i,j}$, $i = 1, 2, \ldots, M$. The term $p_{i,j}$ is called the transition probability from cell j to cell i, and is calculated with a sampling method as given in Zhang98. For all M generalized cells, the transition probabilities construct a transition probability matrix $\mathbf{P}$ of order $M \times M$. Let $\mathbf{p}(n)$ denote the probability distribution of time t_n, so the probability distribution of t_{n+1} is

$$\mathbf{p}(n+1) = \mathbf{P}\mathbf{p}(n) \tag{5}$$

Once $\mathbf{p}(0)$ at time t_0 is given, the subsequent evolution is simply given by

$$\mathbf{p}(n) = \mathbf{P}^n \mathbf{p}(0) \tag{6}$$

The evolution of the system is changed from simple cell-to-cell mapping to the transition of probability in generalized cell-to-cell mapping and is completely described by (5) or (6), and therefore, is controlled by the transition probability matrix $\mathbf{P}$. Meanwhile, this generalized cell mapping formulation leads to finite Markov chains. The establishment and evolution of the coupled model shows that the system is aperiodic and ergodic and the limit probability distribution exists as $n \to \infty$. Thus, the long-term asymptotic behavior is deterministic under the concept of generalized cell mapping although the individual system state is indeterministic. The climate state of the system is now determined by the limit probability distribution on the chaotic attractor.

4.3 Improved algorithm of generalized cell mapping for the coupled model

As pointed out in Zhang98, cell partition is critical for the method. A reasonable cell number could give a satisfactory result while the computation could easily be carried out. For the 3-dimensional phase space of (2), Zhang98 suggested 1000 regular cells and obtained validated results. In each cell, 16^3 samples were used for sampling.

The coupled model has a 6-dimentional phase space. If a similar sampling method to the atmospheric model is used here, the computation amount will be extremely large due to two factors: 1) the transition probability matrix is of order 10^6 (if a similar partition for $\mathbf{X}$ is used for $\mathbf{T}$); and 2) because of the periodic changing of external forcing (solar radiation), the system evolution can no longer be a stationary Markov chain, and consequently, the matrix $\mathbf{P}$ of each time step of land model should be calculated and stored.

A time and memory saving algorithm for calculating a transition probability matrix of the coupled model is given as follows. With reference to the partition in $\mathbf{X}$ space, we discretize the $\mathbf{T}$ space (4) into 216 cells (6 parts on each direction).

The transition matrix of $\mathbf{X}$ with a given $\mathbf{T}$, which corresponds to the kth cell in the $\mathbf{T}$ space, can be written as

$$\mathbf{P}_X^k = \begin{bmatrix} p_{1,1}^k & p_{1,2}^k & \cdots & p_{1,1000}^k \\ p_{2,1}^k & p_{2,2}^k & \cdots & p_{2,1000}^k \\ \vdots & \vdots & p_{i,j}^k & \vdots \\ p_{1000,1}^k & p_{1000,2}^k & \cdots & p_{1000,1000}^k \end{bmatrix} \tag{7}$$

where the element $p_{i,j}^k$ is the transition probability from cell j to i when $\mathbf{T}$ lies in cell k. Assume $\mathbf{T}$ has its own transition probability matrix

$$\mathbf{P}_T = \begin{bmatrix} q_{1,1} & q_{1,2} & \cdots & q_{1,216} \\ q_{2,1} & q_{2,2} & \cdots & q_{2,216} \\ \vdots & \vdots & q_{l,k} & \vdots \\ q_{216,1} & q_{216,2} & \cdots & q_{216,216} \end{bmatrix} \tag{8}$$

where the element $q_{l,k}$ expresses the one-step transition probability from cell k to cell l. Known from the land model (3), the change of **T** depends on solar radiation, initial **T**, and feedback of **X**. Thus, **T** can be expressed as

$$\mathbf{T} = \mathbf{T}_R + \mathbf{T}_I + \mathbf{T}_X \tag{9}$$

where R, I and X stands for radiation, initial, and **X**, respectively. Once the initial at one time is given, $\mathbf{T}_R$ and $\mathbf{T}_I$ at the next step are determined readily. However, the state of **X** at the next step after transition is not unique. This leads to uncertainty of the next step **T**. Indeed, the transition probability from cell k to l, $q_{l,k}$, equals to the sum of the probabilities of all those **X** cells that can make the next step **T** fall into cell l. For a certain k, therefore, the kth column of $\mathbf{P}_T$ is obtained. Therefore, for different initial **T** cells of an initial distribution, the transition probability matrix $\mathbf{P}_T$ is obtained. Insodoing, a joint transition probability matrix of **X** and **T** can be written out using the knowledge of probability theory:

$$\mathbf{P}_{XT} = \begin{bmatrix} \mathbf{P}_X^1 q_{1,1} & \mathbf{P}_X^2 q_{1,2} & \cdots & \mathbf{P}_X^{216} q_{1,216} \\ \mathbf{P}_X^1 q_{2,1} & \mathbf{P}_X^2 q_{2,2} & \cdots & \mathbf{P}_X^{216} q_{2,216} \\ \vdots & \vdots & \mathbf{P}_X^k q_{l,k} & \vdots \\ \mathbf{P}_X^1 q_{216,1} & \mathbf{P}_X^2 q_{216,2} & \cdots & \mathbf{P}_X^{216} q_{216,216} \end{bmatrix} \tag{10}$$

Similar rules as (5) and (6) can be used to obtain the evolution of the coupled model. The long-term behavior of the coupled system can be investigated by global analysis.

According to the analysis of the algorithm, the actual calculation of $\mathbf{P}_T$ is column by column, which is the same for $\mathbf{P}_{XT}$. The storage of the whole $\mathbf{P}_{XT}$ is avoided.

5. Climate predictability of the simple climate system

The perspective of chaotic climate attractor discussed in previous sections has established the foundation for the climate predictability study. With the introduction of cell mapping global analysis method, the infinite system becomes finite; the individual uncertainty turns into integral certainty. These provide the prerequisite for the study of climate predictability and climate prediction.

As discussed in the previous section, there exists a limit probability distribution for the coupled system. The limit probability distribution stands for the final system states when all the initial information has been completely lost. Predictability is to study the period when the initial information still has effects on the system evolution. Ulteriorly, predictability limit is straight forwardly defined as the time period before the system reaches its limit probability distribution on the climate attractor.

Zhang98 has applied the cell mapping method to get the atmospheric model's day-to-day predictability limit, which has been shown as 15–31 days corresponding to different external parameters. In this paper, the atmospheric predictability is investigated within the environment of the coupled model, so do the climate predictability.

Given an initial probability distribution and a convergence criteria

$$\sqrt{\frac{1}{N}\sum_{i=1}^{N}(p_i^{(n+1)} - p_i^{(n)})^2} < \varepsilon, \tag{11}$$

where N is total number of cells and n is time step, the climate probability distribution can be obtained according to Eq. (6) when (11) is satisfied after n iterations. The predictability limit will be $n\tau$, where τ is the time scale of probability transition. For the coupled model, both day-to-day and temporal averaging predictions are studied in this article.

For temporal averaging prediction, for example, the monthly mean prediction of the coupled model is performed following the method in section 4.3. The probability transition of mean T, denoted as $\bar{T}$, is determined by $\bar{T}_R$, $\bar{T}_I$, and $\bar{T}_X$. The term $\bar{T}_R$ is the contribution of average solar radiation in the month, $\bar{T}_I$ is the monthly mean of initial effects on each day, and $\bar{T}_X$ is the feedback of mean X after its transition. So, the transition matrix of $\bar{T}$, and subsequently the joint transition matrix of $\bar{X}$ and $\bar{T}$ can be obtained. The distribution of monthly mean can be predicted with a given initial.

According to the definition of the predictability limit, its actual value will vary with different iteration precision ε. Therefore, predictability limits of multiple ε have been studied in order to get a global understanding. Actually, under the concept of generalized cell mapping, the iteration precision ε is equivalent to the observation precision. High precision ε means small impacts of initial condition can be measured and, therefore, has a longer predictability limit.

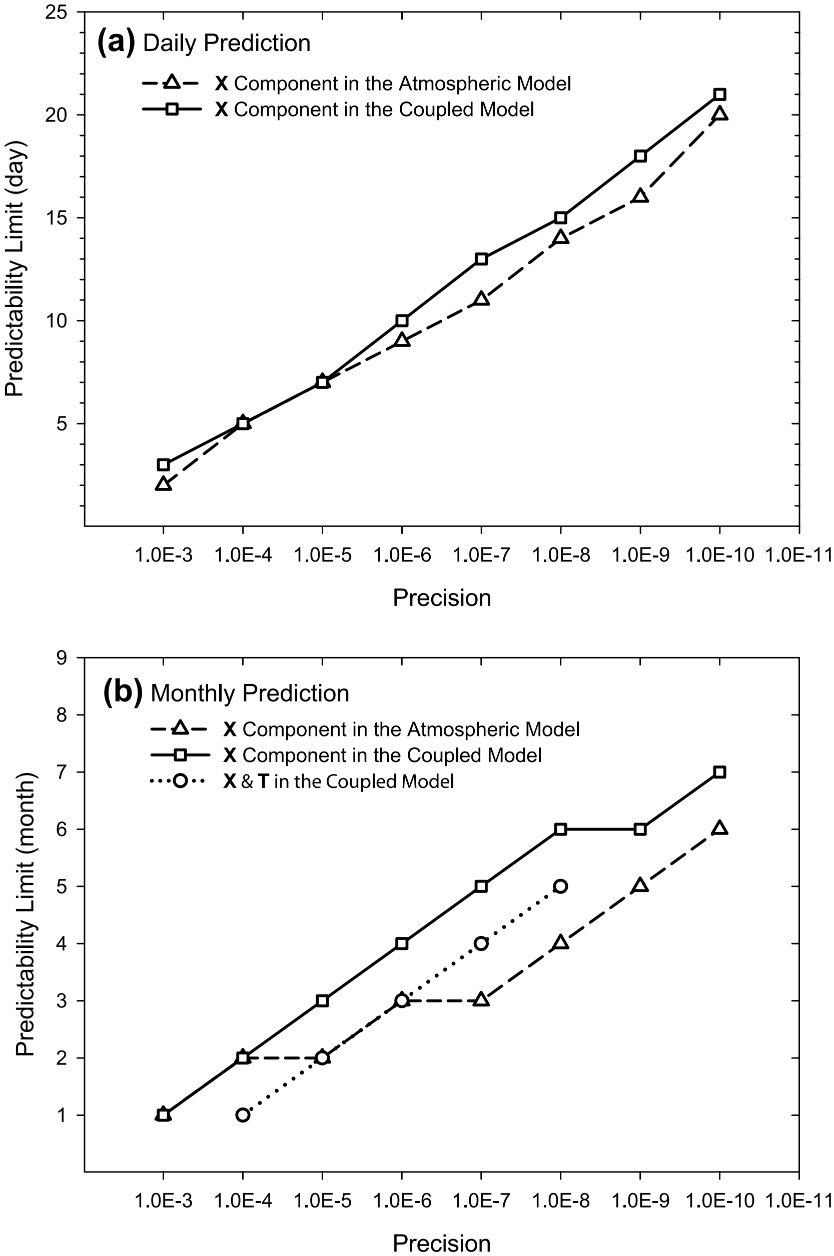

Fig. 3. Daily and monthly predictability limit of different 'observational' errors: **a**) Daily predictability limit of atmospheric variables (**X**) in both the atmospheric and coupled models; **b**) Monthly predictability limit of atmospheric (**X**) and land (**T**) variables in both the atmospheric and coupled models

The atmospheric predictability is investigated separately in both the atmospheric model (Zhang98) and the coupled model (this study). However, the calculating procedure of predictability for the coupled model is different from the atmospheric model. As mentioned before, the periodic solar radiation has been considered as half-year cycles. So, when the root-mean-square error (RMSE) of predicted probability distribution between two days that are half-year apart is less than a given precision ε, the two days' probability distributions are considered identical. In other words, the prediction of the day ahead has already reached the climate state and the day-to-day prediction later on is meaningless. Therefore, the period from initial time to this day is the predictability limit. Figure 3a shows only the atmospheric predictability limit of day-to-day prediction versus precision ε. The results indicate that the atmospheric predictability limit is extended one or two days in the coupled model than in the uncoupled atmospheric model for most precision cases.

Monthly mean atmospheric prediction has also been investigated in both the atmospheric model and the coupled model. With the half-year period of solar radiation in mind, when the RMSE between one month's probability distribution and the month of half-year later is less than a given precision ε, the month's probability distribution is considered being on the climate state. This is the procedure through which the predictability limit of monthly mean prediction is obtained. Figure 3b shows the results of monthly mean prediction. The atmospheric predictability limit in the coupled model is one to three months longer than in the atmospheric model for most precision cases.

Here is why temporal average prediction prolongs the predictability limit from the viewpoint of simple cell mapping. Since the system is deterministic under the concept of simple cell mapping, the system evolution from a given initial cell is completely determined. Thus, the averages of a given time scale fall in definite cells. On the other hand, the averaging operation has smoothed out the variation of system states, which leads to a smaller volume attractor. However, the precision of prediction only needs to be within the observation precision which means the cell size need not to be changed. Therefore, the total number of cells (or states) on the attractor has been lessened, so do the uncertainty. On the contrary, the predictability is increased.

Another conclusion drawn from Fig. 3a and 3b is that the coupling of land model prolongs the atmospheric predictability limit for both day-to-day prediction and monthly mean prediction. The physical mechanism behind this conclusion can be explained like this: The changes of the atmosphere are fast-changing processes, and the changes of the underlying surface temperature are slow-changing processes. The later is relatively a stable component in the coupled system. Although the feedback from the atmosphere is a kind of random perturbation, the underlying surface is functioning as a predominant, stable, and more deterministic component to the atmosphere. Thus, the certainty of the atmosphere is enhanced by the coupling. From the viewpoint of information, the slow-changing underlying surface has longer memory of initial information that prolongs the atmospheric predictability limit.

Figure 3b also shows the results when predicting all the state variable of the coupled system. The predictability limit for the whole coupled system is longer than the atmospheric model at higher observation precisions while it is shorter at lower observation precisions. The reason can also be explained from the viewpoint of cell mapping. There are more cells in the coupled cell space (6-dimensional) than in the atmospheric cell space (3-dimensional). For an initial condition with lower precision, there is less information. Therefore the predictability is lessened.

6. Conclusions and discussion

The coupling of slow-changing land model with the fast-changing atmosphere model helps to get more climate features involved in the study. There are chaotic and stable (periodic) components in the evolution of the coupled system. Three time scales are recognized in the coupled system. A fast process of the atmosphere evolving toward the chaotic attractor determined by the underlying surface temperature, a slow process of the underlying surface temperature affected by solar radiation, and a much slower changing of solar radiation.

The global analysis method, cell mapping, is used to analyze the coupled climate model. The simple cell mapping is a global analysis to round-off error while the generalized cell mapping is a global analysis to observational error. The improved generalized cell mapping method is computationally efficient to be used in the coupled model. Although the evolution of the coupled system is undeterministic due to observational error, it is transformed into a probability transition on a Markov chain by global analysis. The long-term behavior is turned into a deterministic probability distribution on the chaotic attractor, which implies that the climate state can be predicted by means of a combination of dynamics and statistics. There exists a predictability limit determined by observational error in reality.

In terms of climate predictability, the coupling of the land model helps to get longer memory of the initial atmospheric information, and then the predictability limit is extended as a result. Temporal averaging prediction is a way for climate predictions to extend beyond a day-to-day predictability limit.

The coupled simple climate model has the potential to be used in theoretical climate studies, especially for introducing new mathematical theories and methods. As was noticed in this study, the information and fractal theories could be applied in climate prediction study; applied prediction methods based on probability distribution might be studied in this system. There is a wide area for exploration of various climate issues further from this study.

Appendix: Coupling the underlying surface model with the simplified atmospheric model

A.1 Model

The connection between the atmosphere and its underlying surface is established through the energy equilibrium at the interface. Based on the assumption that the solar radiation is absorbed all by the surface, the atmosphere has no affect on the long-wave radiation, and there is no cloud effect and evaporation, then the surface energy equation is simplified as:

$$R_S + R_L = P + A_S \tag{A1}$$

where R_S is solar short-wave radiation, R_L is surface long-wave radiation, P is turbulent heat flux between surface and atmosphere, A_S is heat flux between surface and deep earth. They are given as:

$$R_S(\varphi, t) = \frac{\left|S_0 \cos\left(\varphi + 23.5 \cos \frac{2\pi}{t_R} t\right)\right| + S_0 \cos\left(\varphi + 23.5 \cos \frac{2\pi}{t_R} t\right)}{2} \tag{A2}$$

$$\begin{aligned} R_L(T_{S0}) &= -\sigma T_{S0}^4 = -\sigma[\bar{T}_{S0} + (T_{S0} - \bar{T}_{S0})]^4 \\ &\approx -4\sigma \bar{T}_{S0}^3 T_{S0} + 3\sigma \bar{T}_{S0}^4 \end{aligned} \tag{A3}$$

$$P = \rho C_p C_d |V| (T_{S0} - 2(T)_2) \tag{A4}$$

$$A_S = -\rho_S C_{PS} K_S \frac{\partial T_S}{\partial z} \tag{A5}$$

where the independent variables t and φ are time and latitude ($-90°$ to $90°$), respectively; S_0 is the solar constant; t_R is the yearly period of solar radiation; $+23.5\ \cos(2\pi t/t_R)$ means the year starts from the winter solstice; $T_{S0} = T_S|_{z=0}$ is land surface temperature and $\bar{T}_{S0}$ is land surface eigen temperature; σ is the Stephen-Boltzman constant; ρ, C_P are air density and specific heat, respectively; $|V|$ is absolute wind speed at conventional observation height; C_d is dimensionless dragging coefficient; $(T)_2$ is the model (1) variables $\mathbf{X}$ (see Appendix in Zhang98); ρ_S is soil density; C_{PS} is specific heat of soil; K_S is conductivity coefficient; and z is depth coordinate with positive direction downward.

Applying (A2)–(A5) to (A1), we obtain the boundary condition for land model as

$$\frac{\partial T_S}{\partial z} - H_S T_S = F(\lambda, \theta, t) \tag{A6}$$

where

$$H_S = \frac{1}{\rho_S C_{PS} K_S} (\rho C_P C_d |V| + 4\sigma \bar{T}_{S0}^3) \tag{A7}$$

$$F(\lambda, \theta, t) = -\frac{1}{\rho_S C_{PS} K_S} (2\rho C_P C_d |V| (T)_2 + R_S + 3\sigma \bar{T}_{S0}^4) \tag{A8}$$

The soil temperature T_S is considered satisfying linear thermal conductive equation with the third boundary conditions:

$$\begin{cases} \frac{\partial T_S}{\partial t} - K_S^2 \frac{\partial^2 T_S}{\partial z^2} = 0 \\ T_S(z,t)|_{t=0} = T_S(z,0) \\ \frac{\partial T_S}{\partial z} - H_S T_S = F(\lambda, \theta, t) & \text{when } z = 0 \\ T_S = 0 & \text{when } z = D \end{cases} \tag{A9}$$

where D is the depth of soil temperature annual variation or the thickness of active layer in the ocean.

Assume $T_S = \bar{T}_{S0} T_S'$, $t = \frac{1}{\Omega} t'$, $z = Dz'$, Eq. (A9) is non-dimensioned to get the linear model of soil temperature:

$$\begin{cases} \frac{\partial T_S}{\partial t} - k_S^2 \frac{\partial^2 T_S}{\partial z^2} = 0 \\ T_S(z,t)|_{t=0} = T_S(z,0) \\ \frac{\partial T_S}{\partial z} - h_S T_S = f(\lambda, \theta, t) & \text{when } z = 0 \\ T_S = 0 & \text{when } z = D \end{cases} \tag{A10}$$

where

$$k_S^2 = \frac{K_S^2}{\Omega D^2} \tag{A11}$$

$$h_S = D H_S \tag{A12}$$

$$f(\lambda, \theta, t) = a_1 (T)_2 + a_2 (R_S + 3\sigma \bar{T}_{S0}^4) \tag{A13}$$

$$a_1 = -\frac{2a_0^2 \Omega^2 D \rho C_P C_d |V|}{\rho_S C_{PS} K_S \bar{T}_{S0} R} \tag{A14}$$

$$a_2 = -\frac{D}{\rho_S C_{PS} K_S \bar{T}_{S0}} \tag{A15}$$

By referencing to Guo et al. (1996), an analytical solution to the model (A10) exists as

$$\begin{aligned} T_S(z,t) = &- \int_0^t \frac{k_s}{\sqrt{\pi(t-\tau)}} \Bigg[e^{-\frac{z^2}{4k_S^2(t-\tau)}} \\ &- h_S \int_0^\infty e^{-h_S \eta - \frac{(z+\eta)^2}{4k_S^2(t-\tau)}} d\eta \Bigg] f(\lambda, \theta, \tau) d\tau \\ &+ \frac{1}{2k_S\sqrt{\pi t}} \int_0^D \Bigg[e^{-\frac{(z-\zeta)^2}{4k_S^2 t}} + e^{-\frac{(z+\zeta)^2}{4k_S^2 t}} \\ &- 2h_S \int_0^\infty e^{-h_S \eta - \frac{(z+\zeta+\eta)^2}{4k_S^2 t}} d\eta \Bigg] T_S(\zeta, 0) d\zeta \end{aligned} \tag{A16}$$

A.2 Algorithm for calculating solution (A16)

There are difficulties in calculating T_S from Eq. (A16) because the two infinite integrals in (A16) are difficult to compute. The following gives an algorithm which can be used for calculation. The two integrals are denoted as:

$$I_1 = \int_0^\infty e^{-h_S\eta - \frac{(z+\eta)^2}{4k_S^2(t-\tau)}} d\eta \tag{A17}$$

$$I_2 = \int_0^\infty e^{-h_S\eta - \frac{(z+\zeta+\eta)^2}{4k_S^2 t}} d\eta \tag{A18}$$

For I_1, let $\xi = \frac{z+\eta}{2k_S\sqrt{t-\tau}} + k_S h_S\sqrt{t-\tau}$ and do transformation, then

$$I_1 = 2k_S\sqrt{t-\tau}e^{h_S z + k_S^2 h_S^2(t-\tau)}\left[\int_0^\infty e^{-\xi^2}d\xi - \int_0^{\frac{z}{2k_S\sqrt{t-\tau}}+k_S h_S\sqrt{t-\tau}} e^{-\xi^2}d\xi\right] \tag{A19}$$

Using the probability integral $\Phi(x) = \int_0^x e^{-\xi^2}d\xi$, we get

$$I_1 = 2k_S\sqrt{t-\tau}e^{h_S z + k_S^2 h_S^2(t-\tau)} \left[\frac{\sqrt{\pi}}{2} - \Phi\left(\frac{z}{2k_S\sqrt{t-\tau}} + k_S h_S\sqrt{t-\tau}\right)\right] \tag{A20}$$

For I_2, let $S = \frac{z+\zeta+\eta}{2k_S\sqrt{t}} + k_S h_S\sqrt{t}$, and do similar deduction as for I_1, we get

$$I_2 = 2k_S\sqrt{t}\, e^{h_S(z+\zeta)+k_S^2 h_S^2 t}\left[\frac{\sqrt{\pi}}{2} - \Psi\left(\frac{z+\zeta}{2k_S\sqrt{t}} + k_S h_S\sqrt{t}\right)\right] \tag{A21}$$

Applying (A20) and (A21) to (A16), we get

$$\begin{aligned} T_S(z,t) = &-\frac{k_S}{\sqrt{\pi}}\int_0^t \frac{1}{\sqrt{(t-\tau)}} e^{-\frac{z^2}{4k_S^2(t-\tau)}} f(\lambda,\theta,\tau)d\tau \\ &+ k_S^2 h_S e^{h_S z}\int_0^t e^{k_S^2 h_S^2(t-\tau)} f(\lambda,\theta,\tau)d\tau \\ &- \frac{2k_S^2 h_S}{\sqrt{\pi}} e^{h_S z}\int_0^t e^{k_S^2 h_S^2(t-\tau)}\Phi\left(\frac{z}{2k_S\sqrt{t-\tau}} + k_S h_S\sqrt{t-\tau}\right) f(\lambda,\theta,\tau)d\tau \\ &+ \frac{1}{2k_S\sqrt{\pi t}}\int_0^D e^{-\frac{(z-\zeta)^2}{4k_S^2 t}} T_S(\zeta,0)d\zeta \\ &+ \int_0^D e^{-\frac{(z+\zeta)^2}{4k_S^2 t}} T_S(\zeta,0)d\zeta \\ &- h_S\int_0^D e^{h_S(z+\zeta)+k_S^2 h_S^2 t} T_S(\zeta,0)d\zeta \\ &+ \frac{2h_S}{\sqrt{\pi}}\int_0^D e^{h_S(z+\zeta)+k_S^2 h_S^2 t}\Psi\left(\frac{z+\zeta}{2k_S\sqrt{t}} + k_S h_S\sqrt{t}\right) T_S(\zeta,0)d\zeta \end{aligned} \tag{A22}$$

For practical calculation, the integrals in the above equation should be substituted by summation. Through discretizing the integral range t and D into n and m parts, respectively, when $\Delta t = t/n$ and $\Delta D = D/m$ are small enough, the integral intermediate value theorem is used for (A22). Now we have:

$$T_S(z,t) = \sum_{i=1}^{n}[F_1(z,t,\tau_i)f(\lambda,\theta,\tau_i)] + \sum_{i=1}^{m}[F_2(z,t,\zeta_i)T_S(\zeta_i,0)] \tag{A23}$$

where

$$\begin{aligned} F_1(z,t,\tau_i) = &-\frac{2k_S}{\sqrt{\pi}}\left(\sqrt{i\Delta t} - \sqrt{(i-1)\Delta t}\right)e^{-\frac{z^2}{4k_S^2(t-\tau_i)}} \\ &+ \frac{2k_S^2 h_S\Delta t}{\sqrt{\pi}}\left[\frac{\sqrt{\pi}}{2} - \Phi\left(\frac{z}{2k_S\sqrt{t-\tau_i}} + k_S h_S\sqrt{t-\tau_i}\right)\right]e^{h_S z + k_S^2 h_S^2(t-\tau_i)} \end{aligned} \tag{A24}$$

$$\begin{aligned} F_2(z,t,\zeta_i) = &-\frac{\Delta D}{2k_S\sqrt{\pi t}}\left(e^{-\frac{(z-\zeta_i)^2}{4k_S^2 t}} + e^{-\frac{(z+\zeta_i)^2}{4k_S^2 t}}\right) \\ &- \frac{2h_S\Delta D}{\sqrt{\pi}}\left[\frac{\sqrt{\pi}}{2} - \Psi\left(\frac{z+\zeta_i}{2k_S\sqrt{t}} + k_S h_S\sqrt{t}\right)\right]e^{h_S(z+\zeta_i)+k_S^2 h_S^2 t} \end{aligned} \tag{A25}$$

$$(i-1)\Delta t < \tau_i < i\Delta t \quad \text{and} \quad (i-1)\Delta D < \zeta_i < i\Delta D \tag{A26}$$

A.3 Coupling with the atmospheric model (1)

The land model can be easily coupled with the atmospheric model (1) through the temperature continuity condition at the interface:

$$(T)_4 = T_s|_{z=0} - \hat{T} \tag{A27}$$

where $\hat{T}$ is environment temperature, $T_s|_{z=0}$ is the land surface temperature calculated from land model (3), $(T)_4$ is the external forcing required by the atmospheric model. Here we select similar base functions as in Appendix of Zhang98:

$$P_2^0 = \frac{1}{2}(3\cos^2\theta - 1), P_4^2 = \frac{15}{2}(-7\cos^4\theta + 8\cos^2\theta - 1) \tag{A28}$$

and suppose

$$(T)_4 = (T_1)_4 \cdot 10P_2^0 + (T_2)_4 P_4^2\cos 2\lambda + (T_3)_4 P_4^2\sin 2\lambda \tag{A29}$$

then we can get

$$(T_1)_4 = \frac{\int_0^{2\pi}\int_0^{\pi}(T_s|_{z=0} - \hat{T})P_2^0\sin\theta\, d\theta d\lambda}{20\pi\int_0^{\pi}(P_2^0)^2\sin\theta\, d\theta} \tag{A30}$$

$$(T_2)_4 = \frac{\int_0^{2\pi}\int_0^{\pi}(T_s|_{z=0} - \hat{T})P_4^2\cos 2\lambda\sin\theta\, d\theta d\lambda}{\pi\int_0^{\pi}(P_4^2)^2\sin\theta\, d\theta} \tag{A31}$$

$$(T_3)_4 = \frac{\int_0^{2\pi}\int_0^{\pi}(T_s|_{z=0} - \hat{T})P_4^2\sin 2\lambda\sin\theta\, d\theta d\lambda}{\pi\int_0^{\pi}(P_4^2)^2\sin\theta\, d\theta} \tag{A32}$$

Through (A30)–(A32), the two models are coupled. When a set of initial land surface temperature $(T)_4$ is given, an approximate set of initial soil temperature for different depth can be derived by utilizing a lapse rate of soil temperature, γ_s, which is set as a constant.

A.4 Constants and parameters

$S_0 = 9.57391\times10^7\,\mathrm{J\,m^{-2}\,s^{-1}}$

$\bar{T}_{S0} = 2.98816\times10^3\,\mathrm{K}$

$C_d = 2.8\times10^{-2}$

$\hat{T}_1 = -261.0\,\mathrm{K}$

$\hat{T}_2 = -20.0\,\mathrm{K}$

$\hat{T}_3 = 5.0\,\mathrm{K}$

$|V| = 10\,\mathrm{m\,s^{-1}}$

$D = 400\,\mathrm{m}$

$\gamma_s = 2.0\times10^{-2}\,\mathrm{K\,m^{-1}}$

$\rho = 1.2923\,\mathrm{kg\,m^{-3}}$

$C_P = 1.0061\times10^3\,\mathrm{J\,kg^{-1}\,K^{-1}}$

$\rho_s = 1.0\times10^3\,\mathrm{kg\,m^{-3}}$

$C_{PS} = 4.18684\times10^3\,\mathrm{J\,kg^{-1}\,K^{-1}}$

$K_S = 1.17399\times10^1\,\mathrm{J\,m^{-2}\,s^{-1}\,K^{-1}}$

$(\bar{T}_1)_4 = 345.1\,\mathrm{K}$

$(\bar{T}_2)_4 = 24.0\,\mathrm{K}$

$(\bar{T}_3)_4 = -388.6\,\mathrm{K}$

Acknowledgements

The study was supported by the Chinese State Key Basic Research Program: Climate Dynamics and Prediction Theories.

Thanks to the reviewer's constructing comments that helped the structuring of this paper.

References

Charney JG, Fleaglem RG, Lally VE, Riehl H, Wark DQ (1966) The feasibility of a global observation and analysis experiment. Bull Amer Meteor Soc 47: 200–220

Charney JG, Shukla J (1980) Predictability of monsoons. In: Sir James Lighthill, Pearce RP (eds) Monsoon dynamics. Cambridge University Press

Chou JF (1983) The decay of the influence of initial fields and some properties of their operations. Acta Meteor Sinica 41: 385–392 (in Chinese with English abstract)

Chou JF (1986) Long-range numerical weather prediction. Beijing: Meteorological Press, pp 329 (in Chinese)

Chou JF (1987) Some generalized properties of the atmospheric model in H-space, R-space, point mapping, cell mapping. Proceedings of International Summer Colloquium on Nonlinear Dynamics of the Atmosphere. Beijing: Science Press. 10–20 Aug. 1986, 187–189

Chou JF (1989) Predictability of the atmosphere. Adv Atmos Sci 6: 336–346

Chou JF (1995) Global analysis to the atmospheric dynamic equations. J Beijing Meteorological College 1: 1–12

Guo BR, Jiang JM, Fan X, Zhang H, Chou JF (1996) Nonlinear character of climate system and prediction theory. Beijing: Meteorological Press, pp 254 (in Chinese)

Hsu CS (1980) A theory of cell-to-cell mapping dynamical system. ASME J Appl Mech 47: 931–939

Hsu CS, Guttalu RS (1980) An untravelling algorithm for global analysis of dynamical systems: An application of cell-to-cell mapping. ASME J Appl Mech 47: 940–948

Hsu CS (1981) A generalized theory of cell-to-cell mapping for nonlinear dynamical systems. ASME J Appl Mech 48: 634–642

Hsu CS (1982) A probabilistic theory of nonlinear dynamical systems based on cell state space concept. ASME J Appl Mech 49: 895–902

Hsu CS, Guttalu RS, Zhu WH (1982) A method of analyzing generalized cell mapping. ASME J Appl Mech 49: 885–894

Hsu CS (1987) Cell-to-cell mapping – a method of global analysis for nonlinear system. New York: Springer

Lorenz EN (1963) Deterministic nonperiodic flow. J Atmos Sci 20: 130–141

Lorenz EN (1965) A study of the predictability of a 28-variable atmospheric model. Tellus 17: 321–333

Lorenz EN (1969) The predictability of a flow which possesses many scales of motion. Tellus 21: 209–307

Lorenz EN (1982) Atmospheric predictability experiments with a large numerical model. Tellus 34: 505–513

Lorenz EN (1984) Irregularity: a fundamental property of the atmosphere. Tellus 36A: 98–110

Nicolis C (1990) Chaotic dynamics, Markov processes and climate predictability. Tellus 42A: 401–412

Shukla J (1981) Dynamical predictability of monthly means. J Atmos Sci 38: 2547–2572

Smagorinsky J (1969) Problems and promises of deterministic extended range forecasting. Bull Amer Meteor Soc 50: 286–311

Thompson JMI, Stewart HB (1986) Nonlinear dynamics and chaos. Chichester: John Wiley and Sons

Zhang H, Fan X, Xu M, Chou JF (1998) Application of a global analysis method to a simplified climate model. Theor Appl Climatol 61: 103–111

Authors' addresses: Xingang Fan (e-mail: xfan@gi.alaska.edu), 903 Koyukuk Dr., P.O. Box 757320, Fairbanks, AK 99775-7320, USA; Ji-Fan Chou, Department of Atmospheric Sciences, Lanzhou University, Lanzhou, China 730000; Bing-Rong Guo, Department of Mathematics, Wuhan University, Wuhan, China 430072; Martha D. Shulski, Geophysical Institute, University of Alaska Fairbanks, Fairbanks, AK 99775, USA.